Design and Performance of Code Tracking for the GPS M Code Signal

John W. Betz, *The MITRE Corporation*

BIOGRAPHY

John W. Betz is a Consulting Engineer at The MITRE Corporation. He received a Ph.D. in Electrical and Computer Engineering from Northeastern University. His work involves development and analysis of signal processing for communications, navigation, radar, and other applications. He developed the Binary Offset Carrier modulation for the GPS M code signal. During 1998 and 1999, he led the GPS Modernization Signal Design Team's Modulation and Acquisition Design Subteam, contributing to many aspects of the signal design and evaluation. He has authored many technical papers and reports on theory and applications of signal processing.

ABSTRACT

The binary offset carrier (BOC) modulation of the new GPS military ranging signal, the M code signal, provides essential benefits in many respects. Because of this signal's differences from conventional ranging signals, M code receiver performance also benefits from some changes to conventional designs. Extensive analysis, simulation, and hardware experimentation have yielded useful insights in receiver design; some of the key insights are provided in this paper. A discriminator design approach is described based on theoretically developed S curves and predictions of code tracking accuracy, and used to configure the experimental hardware. It is seen that the design approach must be somewhat different from that used for receivers of C/A code and Y code signals, in order to take advantage of the unique characteristics of BOC modulations. Theoretical expressions are presented that describe performance of despreading and code tracking the M code signal's BOC(10,5) modulation using a delay-locked loop with noncoherent early-late discriminator. Simple algebraic approximations are also provided. Theoretical predictions of signal-to-noise ratio and code tracking accuracy in white noise are compared with measured results, demonstrating the utility of the design approach and close comparison between theoretical predictions and measurements. Finally, the effect of front-end bandwidth on receiver performance is assessed.

INTRODUCTION

During 1998 and 1999, the GPS Military Signal Design Team (GMSDT), led by the GPS Joint Program Office (JPO), produced a recommended design of the new military signal—the M code signal—for the L1 and L2 bands. [1] summarizes the resulting design recommendation; development of transmission capability in satellites is beginning, and exploration of receiver designs has begun.

Many design criteria involving different aspects of performance and addressing compatibility with existing GPS signals were employed in selecting the best modulation design, consistent with the currently allocated frequency spectrum. Since novel modulation designs were being considered, it was important that appropriate receiver processing was employed in the evaluations and design studies that considered performance of receiver processing.

Traditionally, theory and practice for GPS receiver design has focused on conventional modulations using a rectangular spreading symbol, producing sinc-squared spectra. Extensive experience has been obtained [2, 3] in designing receivers for these signals, with emphasis on situations involving white noise and where the receiver's front-end bandwidth is much wider than the signal's null-to-null bandwidth.

For various reasons, this available theory and practice do not apply to receiver processing of BOC modulations. The spreading symbols are not simple rectangles, but rather segments of a square wave [1, 4], leading to novel shapes of spectra and correlation functions, including a much sharper peak in the correlation function. The discriminator spacing must be narrow enough to fit the peak of the correlation function. Also, the M code receiver's front-end bandwidth is not much wider than the signal bandwidth in many cases of interest. It has been shown recently [5] that even the

theory of tracking conventional modulations must be modified when the discriminator is not spacing-limited; i.e., when the product of the receiver front-end bandwidth and the discriminator spacing is less than π. Since the M code receiver is not spacing-limited and is not processing conventional signals with rectangular spreading symbols and sinc-squared modulations, new theory and practice are warranted.

Since acquisition of the M code signal is addressed elsewhere, including [6], this paper does not dwell on acquisition of the M code signal. Furthermore, once the receiver has performed code tracking and despreading, carrier tracking and data demodulation are similar in concept to that in conventional receivers—well-known but different details are needed due to the convolutional encoding and the different data rates. Consequently, the remaining areas of signal processing where M code receiver processing most differs from that of conventional receivers involves code tracking and despreading.

Fortunately, new theory has recently been developed [7, 8] to predict code tracking accuracy when the signal spectrum has arbitrary shape and the receiver front-end bandwidth is not necessarily much wider than the signal bandwidth. Although this new theory also does not require the noise to be white, application of the theory in this paper involves only white noise; other applications can be found in [9, 10].

This theory was used during the M code signal design process to guide design of hardware for demonstrating receiver performance, as well as to predict experimental performance. This paper presents the theory used in designing the hardware testbed to process the M code signal, and to predict performance. Next it provides numerical results obtained theoretically, and then simple approximate expressions that describe performance. Some opportunities for errors in analysis and measurement are identified and illustrated. Measurements from experimental hardware are then compared with theoretical predictions. Then the effect of front-end bandwidth on receiver performance is considered. Finally, the results and their implications are summarized.

SUMMARY OF THEORY

As introduced in [4], BOC modulations are described by two parameters: subcarrier frequency and spreading code rate. For GPS it is beneficial for both of these quantities to be integer multiples of the standard GPS clock frequency of 1.023 MHz. However, for conciseness, the designation of BOC modulations for GPS does not use full precision. For example, the BOC(10,5) modulation selected for the M code signal actually has subcarrier frequency 10.23 MHz and code rate of 5.115 MHz.

The normalized power spectral density of a baseband signal with BOC modulation having subcarrier frequency f_s and spreading code rate f_c is given by [4]

$$G_s(f) = G_{\mathrm{BOC}(f_s,f_c)}(f) = f_c \left(\frac{\sin\left(\frac{\pi f}{2f_s}\right)\sin\left(\frac{\pi f}{f_c}\right)}{\pi f \cos\left(\frac{\pi f}{2f_s}\right)} \right)^2, \quad (1)$$

and the resulting spectrum for BOC(10,5) is plotted in Figure 1.

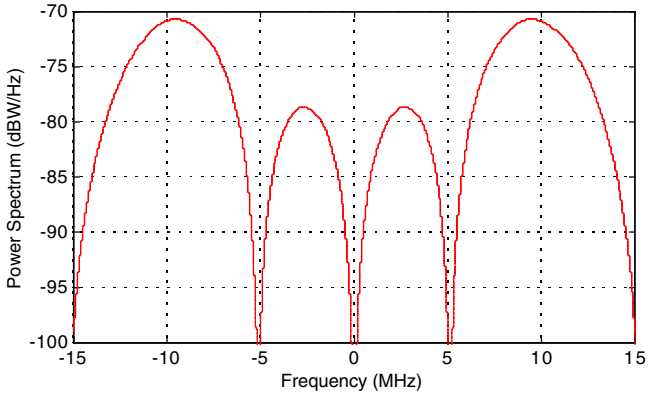

Figure 1. Power Spectral Density of M Code Signal at 1 W

In general, the autocorrelation function of a BOC modulation is not readily expressed in closed form. When the signal is ideally bandlimited to complex bandwidth β_r, the autocorrelation function is given by

$$R_s(\tau) = \int_{-\beta_r/2}^{\beta_r/2} G_s(f) e^{i2\pi f\tau} d\tau. \quad (2)$$

Normalized correlations (i.e., with the maximum value normalized to unity) of the M code modulation, computed with different complex bandwidths, are shown in Figure 2. Since the plots are symmetric in delay, only one side is plotted in order to portray more detail. Normalized magnitude-squared versions of the same data are portrayed in Figure 3. While the main peak of the infinite-bandwidth correlation is slightly sharper than that of the bandlimited correlations, the shapes of the correlations are similar for 30 MHz and 24 MHz bandwidth. In contrast, the sidelobe structure for 20 MHz bandwidth correlation differs somewhat from that of the wider bandwidth correlations. Correlation losses associated with the bandlimiting are discussed in a subsequent section of this paper.

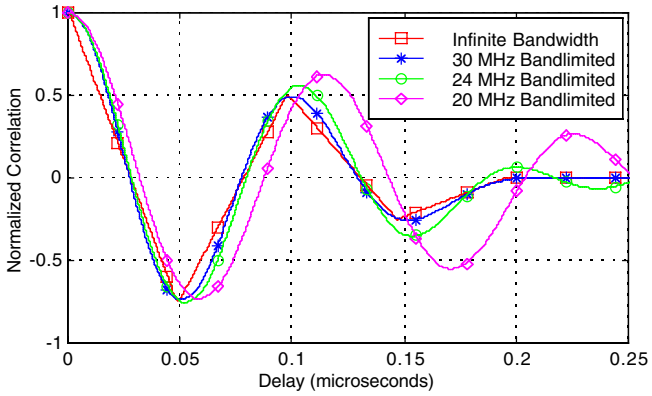

Figure 2. M Code Signal Correlations with Different Front-End Bandwidths

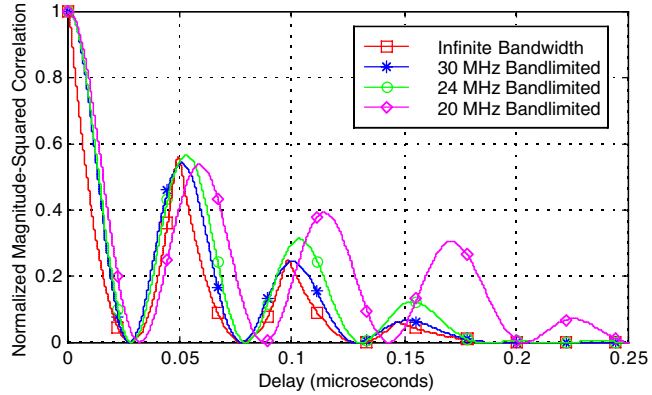

Figure 3. Magnitude-Squared M Code Signal Correlations with Different Front-End Bandwidths

The S-curve for a discriminator using noncoherent early-late processing (NELP) with early-to-late spacing of Δ seconds is given by [11]

$$S(\varepsilon) = \left|R_s(\varepsilon - \Delta/2)\right|^2 - \left|R_s(\varepsilon + \Delta/2)\right|^2 \tag{3}$$

where ε is the error in the signal's time of arrival, and the correlations in (3) are assumed normalized. The discriminator gain is defined as the slope of the S curve at $\varepsilon = 0$,

$$\gamma = \left.\frac{dS(\varepsilon)}{d\varepsilon}\right|_{\varepsilon=0}. \tag{4}$$

The discriminator gain is thus implicitly a function of front-end bandwidth and early-late spacing.

As discussed in [12], breaklock performance of code tracking loops for BOC modulations is enhanced by the use of very-early/very-late processing, or some equivalent form of processing to ensure that the main correlation peak is tracked. Very-early/very-late processing uses additional, widely-spaced correlator taps, along with an algorithm that compares magnitudes at the various taps over time, in order to detect tracking of a correlation function sidelobe, and move the tracking back to the main peak. The performance assessment in this paper, however, considers small errors which are unaffected by very-early/very-late processing, so it need not be considered in the performance analysis here, although it is useful for robust performance.

For first-order performance analysis, model the receiver filter by an ideal rectangular transfer function with complex bandwidth β_r. Denote the received signal power over infinite signal bandwidth by C (units of W), the power spectral density of the noise by N_0 (units of W/Hz). Let the early-late spacing be Δ (units of s), the correlation integration time within the receiver by T (units of s), and B_L (units of Hz) be the one-sided noise equivalent bandwidth of the code tracking loop in Hz. When code tracking errors are small so that a linearized analysis applies, the variance of the code tracking error for NELP (in units of seconds squared) given by substituting (1) into [7, 8]

$$\sigma^2_{\text{NELP}} = \frac{B_L\left(1 - 0.25 B_L T\right)\int_{-\beta_r/2}^{\beta_r/2} G_s(f)\sin^2(\pi f\Delta)\,df}{\frac{C}{N_0}\left(2\pi\int_{-\beta_r/2}^{\beta_r/2} f G_s(f)\sin(\pi f\Delta)\,df\right)^2} \times\left[1 + \frac{\int_{-\beta_r/2}^{\beta_r/2} G_s(f)\cos^2(\pi f\Delta)\,df}{T\frac{C}{N_0}\left(\int_{-\beta_r/2}^{\beta_r/2} G_s(f)\cos(\pi f\Delta)\,df\right)^2}\right]. \tag{5}$$

The term in square brackets reflects the squaring loss suffered from use of noncoherent processing.

Also, for small loop bandwidth, a lower bound on code tracking error in white noise for fixed front-end bandwidth is independent of discriminator spacing and given by [7, 8]

$$\sigma^2_{\text{LB}} = \frac{B_L}{(2\pi)^2\frac{C}{N_0}\beta^2_{\text{rms}}} \tag{6}$$

where β_{rms} is the RMS bandwidth (in Hz) of the bandlimited signal, defined by

$$\beta^2_{\text{rms}} = \int_{-\beta_r/2}^{\beta_r/2} f^2 G_s(f)\,df. \tag{7}$$

Observe that (7) combines two separate effects of bandlimiting the signal to complex bandwidth β_r: the loss of signal power, and the loss of higher-frequency content that sharpens the correlation. To separate these effects, define the correlation loss due to bandlimiting to β_r as

$$\lambda = \int_{-\beta_r/2}^{\beta_r/2} G_s(f)\,df, \tag{8}$$

so that $\lambda^{-1}G_s(f)$ has unit area over the front-end bandwidth (and the corresponding correlation function is normalized). Then (6) can be rewritten

$$\sigma_{\mathrm{LB}}^2 = \frac{B_{\mathrm{L}}}{(2\pi)^2 \frac{\lambda C}{N_0} \tilde{\beta}_{\mathrm{rms}}^2}, \tag{9}$$

with

$$\tilde{\beta}_{\mathrm{rms}}^2 = \int_{-\beta_{\mathrm{r}}/2}^{\beta_{\mathrm{r}}/2} \lambda^{-1} f^2 G_s(f) df. \tag{10}$$

(9) shows the separate effect of correlation loss and eliminated higher-frequency content of the unit-area power spectrum. The same adjustments can be made in (5).

Multiplying the standard deviations from (5) and (6) by the speed of electromagnetic propagation yields the root mean-squared (RMS) code tracking error in units of meters.

Under the same assumptions and using the definition in (8), the output signal-to-noise ratio (SNR) from noncoherent processing is [13]

$$\rho_{\mathrm{n}} = T \frac{C}{N_0} \lambda + 1, \tag{11}$$

while the output signal-to-noise ratio (SNR) from coherent processing is [13]

$$\rho_{\mathrm{c}} = 2T \frac{C}{N_0} \lambda. \tag{12}$$

The expression (12) relates the performance of despreading when the receiver is tracking carrier phase and demodulating data bits.

THEORETICAL RESULTS, DISCRIMINATOR DESIGN AND PERFORMANCE

S curves for NELP of the M code signal, as defined in (3), are shown for infinite bandwidth in Figure 4. The curves are well-behaved for early-late spacings less than 50 ns, but the slope reverses for early-late spacing between 50 ns and 60 ns. As long as an appropriate form of extended range correlation (see [12], for example) is used to ensure that the main peak of the correlation function is tracked, the shape of the S curve away from the zero crossing point does not describe how the code tracking loop behaves.

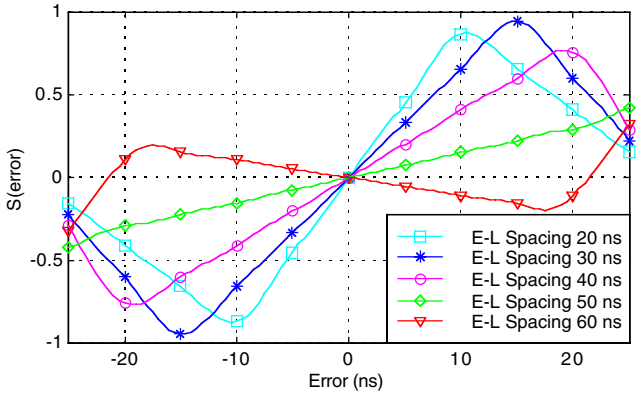

Figure 4. S Curves for NELP with Different Early-Late Spacing and Infinite Front-End Bandwidth

S curves for NELP of the M code signal are shown for 24 MHz front-end bandwidth processing in Figure 5, and for 20 MHz front-end bandwidth processing in Figure 6. Figure 5 indicates the same slope reversal as seen in Figure 4, but this reversal does not appear in Figure 6 because the tighter bandlimiting has changed the shape of the correlation function as seen in Figure 2 and Figure 3, thus changing the shape of the S curve.

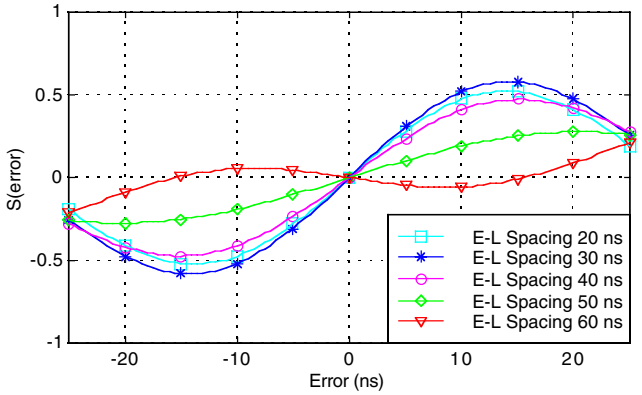

Figure 5. S Curves for NELP with Different Early-Late Spacing and 24 MHz Front-End Bandwidth

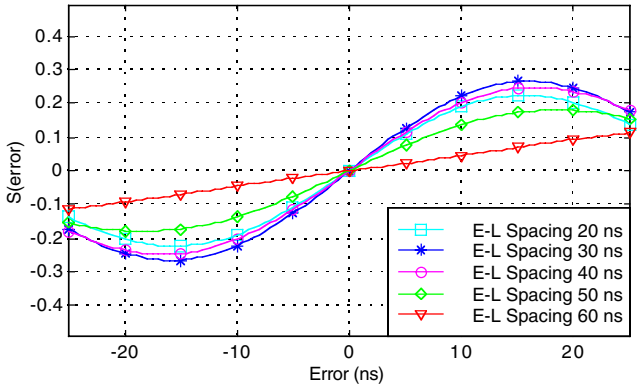

Figure 6. S Curves for NELP with Different Early-Late Spacing and 20 MHz Front-End Bandwidth

Table 1 lists the discriminator gains for different front-end bandwidths and early-late spacings. It will be seen below that the code tracking accuracy for different discriminator designs cannot be inferred from the values of the slopes, since this conventional rule of thumb does not account for effects of front-end bandlimiting, which are important here as discussed in [5, 7, 8].

Table 1. Discriminator Gains

Front-End Bandwidth (MHz)	Early-Late Spacing (ns)	Discriminator Gain (per μs)
Infinite	20	95
Infinite	30	65
Infinite	40	40
Infinite	50	15
Infinite	60	–11
24	20	59
24	30	64
24	40	49
24	50	21
24	60	–10
20	20	23
20	30	26
20	40	24
20	50	16
20	60	4

To assess code tracking accuracy of different discriminator designs for the M code signal, use a signal carrier power-to-noise-density ratio (C / N_0) of 30 dB-Hz, 20 ms correlation integration time, and one-sided equivalent rectangular bandwidth of the code tracking loop of 1 Hz. The curve labeled "M Code Signal" in Figure 7 shows how the code tracking accuracy, computed using (5), varies with early-late spacing for front-end bandwidth of 24 MHz. The slope reversal that was observed in the discriminator curves in Figure 5 causes the code tracking error to become infinite at early-late spacing near 57 ns, but the error approaches an asymptote for early-late spacings less than 50 ns. This asymptote is given by the curve labeled "M Code Signal Lower Bound," which is computed using the lower bound (6). This lower bound is seen to be a tight bound for early-late spacings of interest. In addition, Figure 7 shows the corresponding code tracking accuracy computed for the Y code signal when its discriminator uses the conventional one chip spacing. For these parameters, the RMS code tracking accuracy of the M code signal is a factor of 2.6 better than that of the Y code signal.

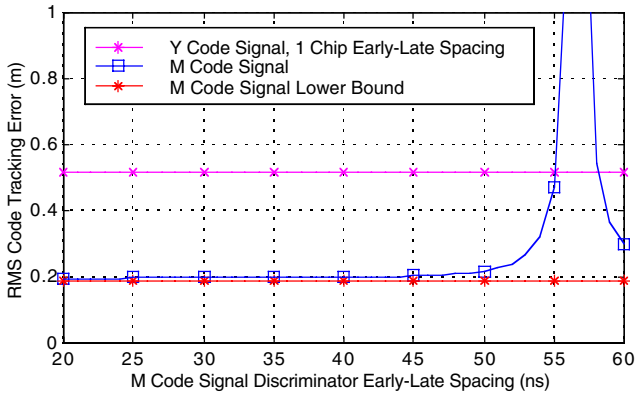

Figure 7. Theoretical Predictions of Code Tracking Error for 20 ms Correlation Integration Time, Receiver Front-End Bandwidth of 24 MHz, and C / N_0 30 dB-Hz

Figure 8 shows the corresponding results for a front-end bandwidth of 20 MHz. The code tracking error for the M code signal increases somewhat with the narrower front-end bandwidth, but still approaches the lower bound computed for this bandwidth. Although the code tracking error increases with wider early-late spacings used, there is no spike as there was in Figure 7. This corresponds to the observation that there is no slope reversal in the discriminator curves portrayed in Figure 6, for the range of discriminator spacings shown. Even though Table 1 shows that the discriminator gain decreases by a factor of 4 as early-late spacing increases from 50 ns to 60 ns for this case with 20 MHz front-end bandwidth, Figure 8 shows that the RMS code tracking error only increases by less than 50%. Again, this supports the observation that discriminator gain does not directly relate to code tracking accuracy for the parameter values of interest to M code receivers.

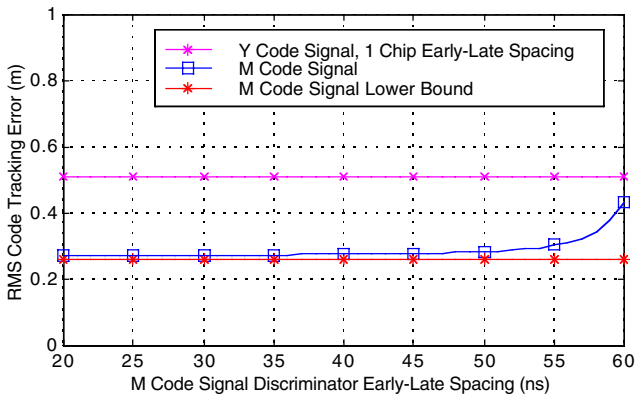

Figure 8. Theoretical Predictions of Code Tracking Error for 20 ms Correlation Integration Time, Receiver Front-End Bandwidth of 20 MHz, and C / N_0 30 dB-Hz

Figure 9 shows results for conditions equivalent to those in Figure 7, except C / N_0 is 20 dB-Hz. For early-late spacing of 50 ns, the code tracking error is beginning to increase a visible amount.

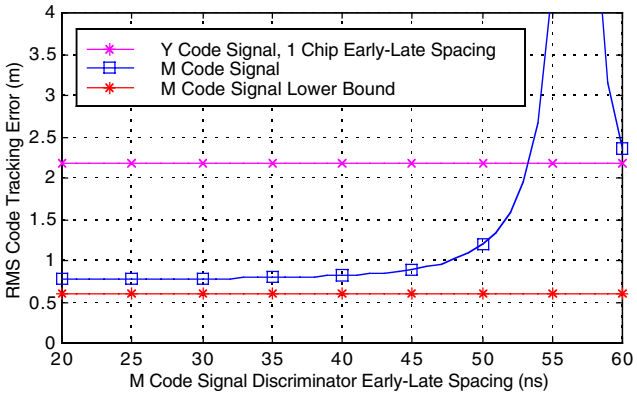

Figure 9. Theoretical Predictions of Code Tracking Error for 20 ms Correlation Integration Time, Receiver Front-End Bandwidth of 24 MHz, and C/N_0 20 dB-Hz

Figure 10 shows results for conditions equivalent to those in Figure 8, except C/N_0 is 20 dB-Hz. For early-late spacing greater than 50 ns, the code tracking error increases a visible amount.

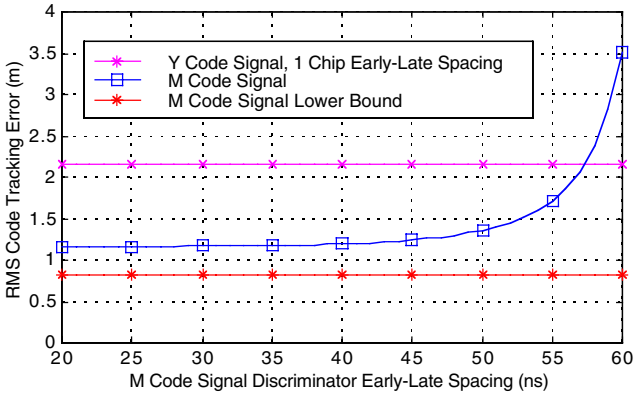

Figure 10. Theoretical Predictions of Code Tracking Error for 20 ms Correlation Integration Time, Receiver Front-End Bandwidth of 20 MHz, and C/N_0 20 dB-Hz

When the correlation integration time is 5 ms and C/N_0 is 30 dB-Hz, the results are very similar to those in Figure 7 and Figure 8, and are not provided here. However, Figure 11 shows the results for the same case as in Figure 7, except the correlation integration time used for the M code signal is 5 ms. The code tracking error increases significantly for early-late spacings greater than 40 ns, due to the increased squaring loss.

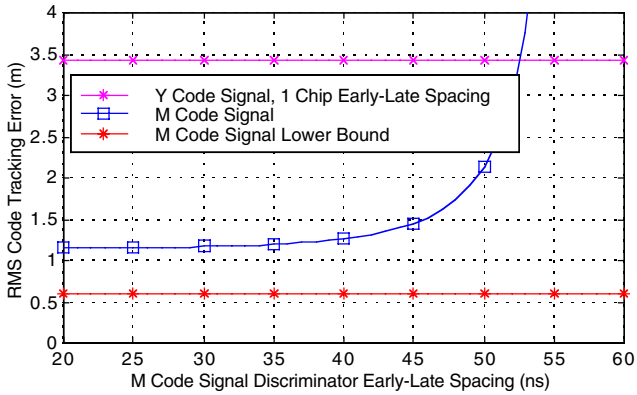

Figure 11. Theoretical Predictions of Code Tracking Error for 5 ms Correlation Integration Time, Receiver Front-End Bandwidth of 24 MHz, and C/N_0 20 dB-Hz

Figure 12 shows the results for the same case as in Figure 8, except the correlation integration time used for the M code signal is 5 ms. The increase in code tracking error with larger early-late spacings is not quite as apparent with the narrower front-end bandwidth. However, the error is somewhat larger than with 20 ms correlation integration time because of the narrower front-end bandwidth.

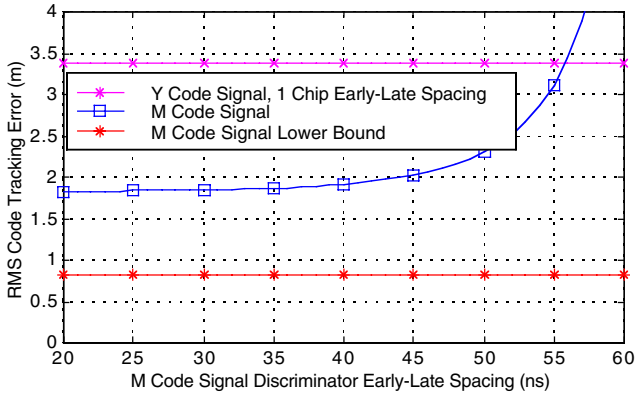

Figure 12. Theoretical Predictions of Code Tracking Error for 5 ms Correlation Integration Time, Receiver Front-End Bandwidth of 20 MHz, and C/N_0 20 dB-Hz

The results provided in Figure 7 through Figure 12 lead to some significant observations. A front-end bandwidth of 24 MHz provides much better performance than a front-end bandwidth of 20 MHz. To ensure robust performance at lower values of C/N_0 and with shorter correlation integration times, the early-late spacing should be 40 ns or less. Also, when C/N_0 is high enough that squaring loss is negligible, and when discriminator spacings suited are appropriate for the M code signal (i.e., 40 ns or less), code tracking error is accurately predicted by the lower bound (6).

APPROXIMATE EXPRESSIONS FOR CORELATION LOSS AND CODE TRACKING ACCURACY

Since evaluating (5) involves numerical integrations, it would be beneficial to have an approximation to (5) that

can be more readily evaluated yet remain accurate over the appropriate range of parameters.

For the BOC(10,5) modulation, the variation of correlation loss (8) with front-end bandwidth β_r can be empirically approximated by two different expressions that apply over different ranges of front-end bandwidths (with β_r expressed in MHz),

$$\lambda \cong \begin{cases} 0.073\beta_r - 0.96, & 16 \text{ MHz} \le \beta_r \le 24.5 \text{ MHz} \\ 0.83, & 24.5 \text{ MHz} < \beta_r \le 30 \text{ MHz}. \end{cases} \quad (13)$$

Figure 13 compares the correlation loss computed using (8) and (13). The approximation is very accurate, having a maximum absolute error of 0.2 dB over the range of bandwidth shown.

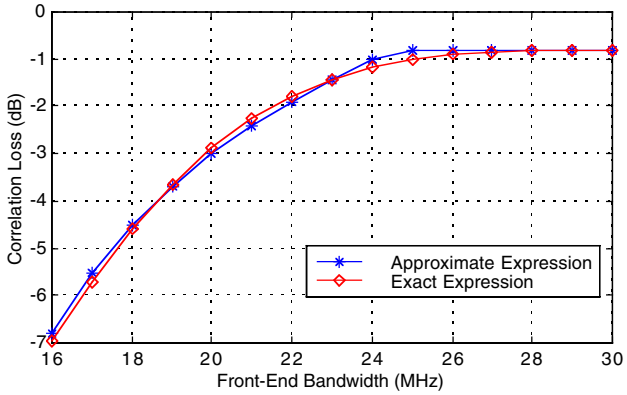

Figure 13. Comparison of Exact Expression (8) and Approximate Expression (13) for M Code Correlation Loss

Variation of the M code signal's RMS bandwidth (7) with front-end bandwidth β_r can also be empirically approximated by two different expressions that apply over different ranges of front-end bandwidths. Similarly, for small discriminator spacings, the squaring loss term in (6) can also be approximated simply. When β_r is expressed in MHz and the other parameters are as defined in the text preceding (5), the M code receiver's code tracking error (5) (in units of seconds squared) can then be approximated, as long as the discriminator spacing is less than 45 ns, as

$$\sigma_M^2 \cong \begin{cases} \dfrac{B_L 10^{-12}}{(2\pi)^2 \dfrac{C}{N_0}(0.66\beta_r - 7.7)^2}\left[1 + \dfrac{1}{(0.073\beta_r - 0.96)T\dfrac{C}{N_0}}\right], \\ \qquad 16 \text{ MHz} \le \beta_r \le 24.5 \text{ MHz} \\ \dfrac{B_L 10^{-12}}{(2\pi)^2 \dfrac{C}{N_0}(0.007\beta_r + 8.4)^2}\left[1 + \dfrac{1}{0.83T\dfrac{C}{N_0}}\right], \\ \qquad 24.5 \text{ MHz} < \beta_r \le 30 \text{ MHz}. \end{cases} \quad (14)$$

Observe that (14) is not a function of the early-late spacing, reflecting the fact that M code discriminators are not spacing-limited.

Figure 14 demonstrates the accuracy of this expression by plotting the exact expression for M code RMS code tracking error (5), converted to units of m, with approximate RMS code tracking error in m obtained from (14). The C/N_0 is 20 dB–Hz, correlation integration time is 20 ms, and the one-sided bandwidth of the code tracking loop is 1 Hz. For these values, the approximation (14) is within 11% of the exact expression (5).

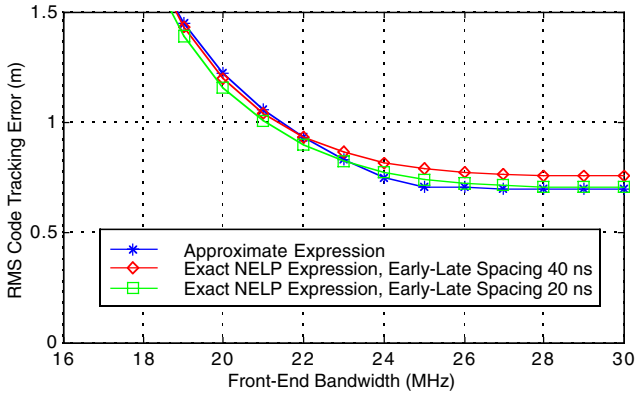

Figure 14. Assessment of Approximate Expression (14) for Code Tracking Error; 20 ms Correlation Integration Time and C/N_0 20 dB-Hz

Figure 15 shows the same case as Figure 14, except with C/N_0 30 dB–Hz. The correlation integration time is 20 ms, and the one-sided bandwidth of the code tracking loop is 1 Hz. For these values, the approximation (14) is within 6% of the exact expression (5).

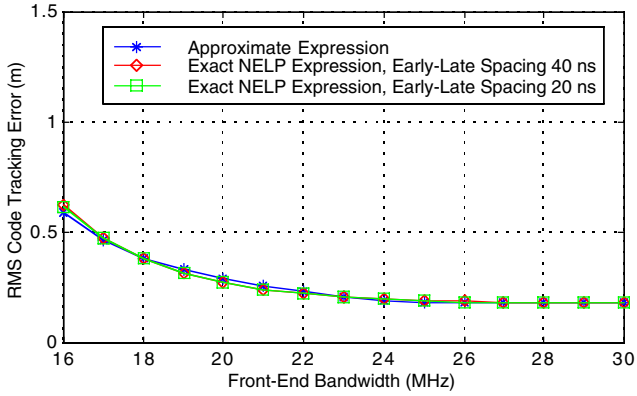

Figure 15. Assessment of Approximate Expression (14) for Code Tracking Error; 20 ms Correlation Integration Time and C/N_0 30 dB-Hz

Figure 16 shows the same case as Figure 14, except with correlation integration time of 5 ms. The approximation (14) is within 16% of the exact expression (5).

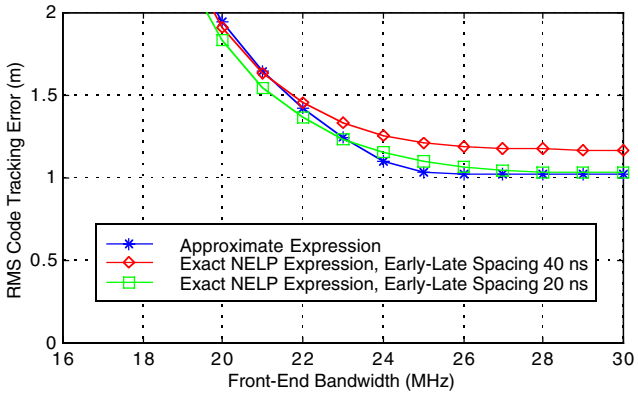

Figure 16. Assessment of Approximate Expression (14) for Code Tracking Error; 5 ms Correlation Integration Time and C / N_0 20 dB-Hz

Figure 17 shows the same case as Figure 15, except with correlation integration time of 5 ms. The approximation (14) is within 9% of the exact expression (5).

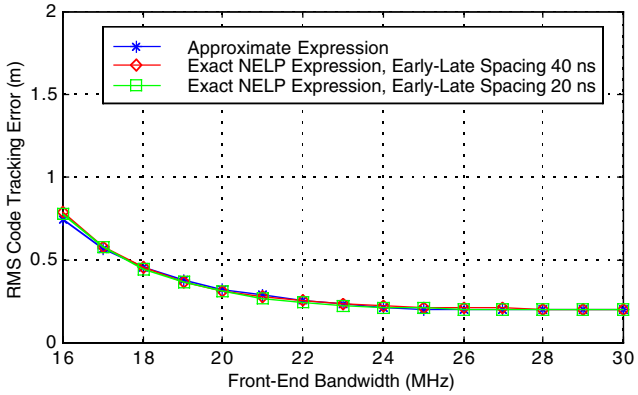

Figure 17. Assessment of Approximate Expression (14) for Code Tracking Error; 5 ms Correlation Integration Time and C / N_0 30 dB-Hz

OPPORTUNITIES FOR ERRONEOUS RESULTS

The subtleties of working with unconventional correlation functions and narrow early-late spacings, and the resulting very small code tracking errors provide opportunities for erroneous results. This section mentions several such opportunities encountered during the initial work on receiving the M code signal, and displays their consequences.

One potential mistake in laboratory measurements or computer simulations involves unknowingly allowing the bandwidth of the code tracking loop to vary. While the expression (5) allows for this bandwidth to change, results like those in the preceding figures are typically evaluated and interpreted under the assumption that the bandwidth of the code loop remains constant.

Well-known results (see [16], for example) show that the equivalent rectangular bandwidth of common code tracking loops is proportional to the loop gain, and that one of the terms that contributes to the loop gain is the discriminator gain. Table 1 shows that as the early-late spacing and front-end bandwidth are changed in exploring different receiver designs, the discriminator gain changes as a result; changing the loop gain and thus causing loop bandwidth to vary. Hence, attempts to produce results like those in this paper with simulations or hardware need to ensure that the loop gain and resulting loop bandwidth are held constant even as the discriminator gain varies due to changes in front-end bandwidth or early-late spacing.

A different potential mistake that can occur in analysis of code tracking error is to neglect the finite front-end bandwidth in computing some of the integrals in (5). If this mistake is made, the predicted error can exhibit interesting but mistaken behavior.

Figure 18 shows of examples these potential mistakes, evaluated with front-end bandwidth equal to 24 MHz, one-sided bandwidth of the code loop of 5 Hz, 20 ms integration time, and C / N_0 of 30 dB-Hz. The curve marked with diamond symbols shows (5) evaluated with loop bandwidth that varies based on discriminator gain, rather than remaining constant. It mistakenly indicates that the code tracking error has a local minimum and then increases for smaller early-late spacings. The curve in Figure 18 marked with square symbols shows a variant of (5) with the limits on the integral in numerator of the first term set to infinity, rather than reflecting the bandlimiting. (Bandlimiting is still employed in the other integrals, and the bandwidth of the code tracking loop is fixed.) This curve also mistakenly shows that there is a local minimum in the code tracking error as the early-late spacing is reduced. The curve marked with asterisks is the expression (5) that accurately reflects bandlimiting and keeps constant the bandwidth of the code tracking loop. This correct result shows that the error monotonically approaches a lower bound, and that code tracking accuracy encounters no penalty (but no enhancement either) from smaller spacings beyond that point.

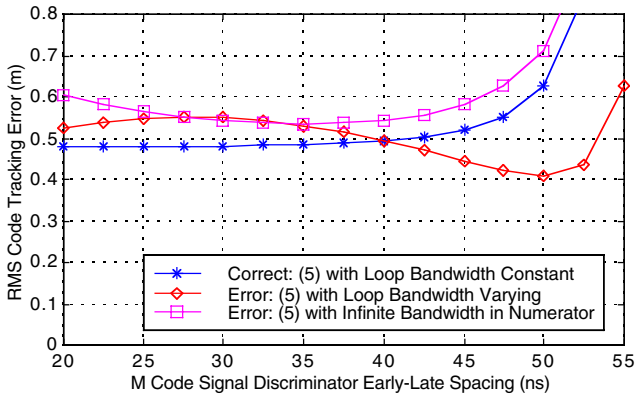

Figure 18. Comparison of Correct and Erroneous Assessments of Code Tracking Error for Receiver Front-End Bandwidth of 24 MHz

COMPARISON OF EXPERIMENTAL AND THEORETICAL RESULTS

Based on the theory and results presented above, a discriminator and code tracking loop were implemented in a hardware testbed. Details of this hardware are provided in [14]. In summary, the hardware generates any of a variety of BOC modulations at carrier frequencies corresponding to L1 or L2, using an arbitrary spreading sequence. The signal generator can be driven by a modified Stanford Telecom Model 7201 GPS constellation simulator to produce appropriate signal dynamics. A Noise/Com UFX programmable noise generator is used to generate white noise, while a Hewlett-Packard E2507B Multiformat Communications Signal Simulator produces interference waveforms at selected power levels.

The receiver performs front-end bandselection filtering of the signal at RF, then downconverts to IF, where the inphase and quadrature channels of the signal are sampled at 65 M (real) samples/s at 12 bits, then digitally downconverted to baseband, with appropriate analog and digital filtering. NELP, appropriately normalized by the prompt correlator value, drives a first-order code tracking loop with one-sided bandwidth of approximately 0.8 Hz. Early-to-late spacing (two-sided) was set to 50 ns.

Power levels of the received signal, thermal noise, and interference waveforms are carefully controlled and monitored, typically within 1 dB. In addition, the code tracking loop's bandwidth is monitored and adjusted as needed to ensure that it remains constant over different conditions.

For the results presented in this paper, the M code signal was received at different carrier power levels in white noise. Analytical predictions were based on the baseband equivalent channel model summarized in Figure 19, drawing upon [15], and using expanded expressions that account for effects of filter magnitude and phase responses on SNR and code tracking error. After power amplification, the transmitted signal is modeled as passing through a triplexer and antenna whose combined frequency response is represented by a four-pole Chebyshev lowpass filter with 0.1 dB ripple and cutoff at ± 14.2 MHz.

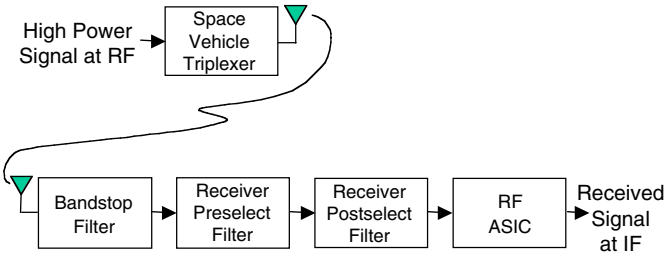

Figure 19. Channel Model for Analytical Predictions

The receiver antenna is modeled by a lowpass fifth-order Butterworth filter with 3 dB points at ± 14.2 MHz. An optional bandstop filter is modeled by a five-pole finite impulse response bandstop filter with 1024 points, whose notch has 3 dB bandwidth of ± 1.975 MHz. The receiver preselect filter is modeled by a third-order Butterworth lowpass filter with 3 dB points of ± 22 MHz, the postselect filter is modeled by a second-order Butterworth lowpass filter with 3 dB points of ± 13.2 MHz, and the frequency response of the RF ASIC is modeled by a third-order Butterworth lowpass filter with 3 dB points of ± 18 MHz. Consequently, the narrowest filter cuts off approximately ± 13 MHz from the center frequency.

The analytical model of the receiver assumes no phase or amplitude equalization of any filter effects, and also assumes that the sampling rate is infinite, omitting losses incurred from aliasing of a sampled binary-valued reference signal in the receiver.

In contrast, the hardware applies essentially no filtering to the transmitted signal, uses filtering in the receiver that cuts off approximately ± 12 MHz from the center frequency, equalizes phase distortion from the receiver filters. The finite sampling rate causes aliasing of the reference signal that contributes to implementation loss.

Hardware measurements were averaged over 120 seconds, after a delay to account for loop settling time. Figure 20 compares theoretically predicted noncoherent output SNR with measured output SNR taken at the magnitude of the prompt correlator tap. Slight implementation losses are evident, with the experimental output SNR slightly less than theoretically predicted.

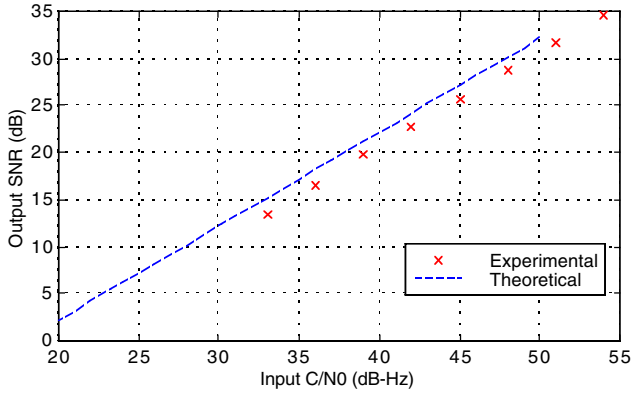

Figure 20. Comparison between Theoretical Predictions and Experimental Measurements of M Code Signal Output SNR

Figure 21 compares theoretically predicted RMS code tracking errors output SNR with measured RMS errors in the code tracking loop SNR. Theoretical predictions match experimental results very closely.

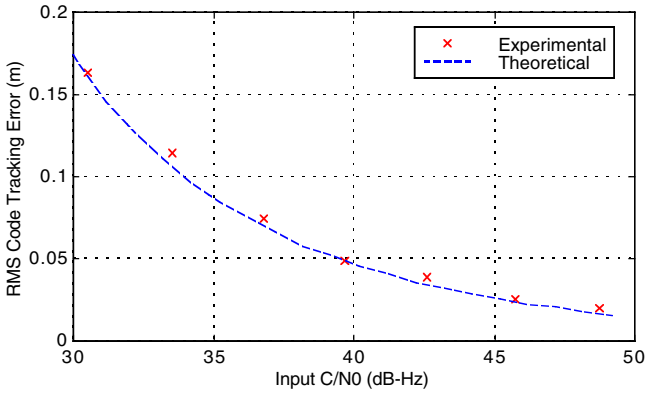

Figure 21. Comparison between Theoretical Predictions and Experimental Measurements of M Code Signal Code Tracking Error

EFFECT OF RECEIVER FRONT-END BANDWIDTH

One topic of obvious practical importance is how wide the front-end bandwidth for an M code receiver should be. Two performance measures are particularly important: correlation loss and code tracking accuracy.

To examine the effect of bandwidth on correlation loss, consider (8) evaluated at different front-end bandwidths. Figure 13 shows the correlation loss from bandlimiting an infinite bandwidth M code signal. There is clearly considerable loss for front-end bandwidths less than 20 MHz. In fact, the correlation loss is reduced by 1.7 dB as the front-end bandwidth is widened from 20 MHz to 24 MHz.

However, the additional benefit of bandwidths greater than 24 MHz is small. In particular, the theory shows that less than 0.3 dB additional signal power is obtained in extending the front-end bandwidth to 28 MHz from 24 MHz, and less than 0.4 dB additional signal power is obtained in extending the front-end bandwidth to 30 MHz from 24 MHz.

For conventional GPS signals there often is significant improvement in code tracking accuracy from extending the front-end bandwidth. However, the M code signal's spectral containment leads to somewhat surprising results in this respect, once the front-end bandwidth is larger than 24 MHz.

Figure 14 through Figure 17 show the effect of front-end bandwidth on code tracking error. For early-late spacings less than 40 ns, extending the front-end bandwidth from 20 MHz to 24 MHz reduces the RMS code tracking error typically by 30%. However, extending the front-end bandwidth further from 24 MHz to 30 MHz only reduces the RMS code tracking error by another 7%. At C/N_0 of 30 dB-Hz, the improvement in RMS code tracking accuracy obtained by extending the front-end bandwidth from 24 MHz to 30 MHz is less than 2 cm.

Clearly, there is substantial benefit in using a front-end bandwidth that passes 24 MHz of signal, but little marginal benefit from bandwidths wider than 24 MHz. In practice, it would be a challenge to obtain any net benefit by extending the bandwidth of signal used to any wider than 24 MHz, since several contributions to implementation losses increase with these wider bandwidths, counteracting the very small theoretical benefits.

DISCUSSION

This paper provides initial guidance and results for the design of receivers for the M code signal's BOC(10,5) modulation. The receiver designs discussed here process the wideband signal, in contrast to single-sideband processing approaches that may be useful in some situations [1].

Conventional concepts of discriminator design need to be adapted for application to the BOC(10,5) modulation. The theory presented here, however, indicates the needed adaptations.

Narrow correlator spacing is important for obtaining the code tracking accuracy inherent in the M code signal's modulation design. S curves are provided for different receiver front-end bandwidths and discriminator spacings, offering insights into choices of design parameters. New theory developed to predict code tracking accuracy of the BOC modulations provides further guidance into receiver designs. Interestingly, a lower bound on code tracking accuracy proves to be a tight bound for parameter choices of interest, providing a simpler expression for predicting code tracking errors. In the example shown, the resulting RMS code tracking accuracy of the M code signal is almost a factor of 2.6 better than obtained using the Y code signal.

Closed-form analytical approximations are provided for predicting both the correlation loss and the code tracking accuracy for reception of the M code signal. These approximations closely match the more precise (but more complicated to evaluate numerically) expressions for these quantities over parameter ranges of interest.

In addition, theoretical predictions of output SNR and code tracking errors in white noise are shown to closely correspond to measured results from a hardware testbed.

Finally, the theory shows that there are significant performance benefits to using receiver front-end bandwidths that pass more than 20 MHz of signal, but vanishing benefits to passing more than 24 MHz of signal bandwidth. In addition, both performance and robustness are improved by selecting early-late spacing of 40 ns or less.

ACKNOWLEDGMENTS

This work was supported by Air Force contract F19628-00-C-001. Thanks to Jeffrey T. Correia for insightful comments and suggestions; to Paul B. Fine and Joseph Leva, who were instrumental in gathering the experimental data used in this paper; and to Dr. Kevin R. Kolodziejski, who co-developed the theory for code tracking accuracy used in this paper.

REFERENCES

1. B. C. Barker, et al., "Details of the GPS M Code Signal," *Proceedings of ION 2000 National Technical Meeting*, Institute of Navigation, January 2000.
2. E. Kaplan (Ed.), *Understanding GPS: Principles and Applications*, Artech House, 1996.
3. B. W. Parkinson and J. J. Spilker, Jr. (Eds.), *Global Positioning System: Theory and Applications, Volume I*, Progress in Astronautics and Aeronautics, Volume 163, 1996.
4. J. W. Betz, "The Offset Carrier Modulation for GPS Modernization," *Proceedings of ION 1999 National Technical Meeting*, Institute of Navigation, January 1999.
5. J. W. Betz and K. R. Kolodziejski, "Extended Theory of Early-Late Code Tracking for a Bandlimited GPS Receiver," to be Published in *Navigation: Journal of The Institute of Navigation*, Fall 2000.
6. P. Fishman and J. W. Betz, "Predicting Performance of Direct Acquisition for the M Code Signal," *Proceedings of ION 2000 National Technical Meeting*, Institute of Navigation, January 2000.
7. K. R. Kolodziejski and J. W. Betz, *Effect of Non-White Gaussian Interference on GPS Code Tracking Accuracy*, The MITRE Corporation Technical Report MTR99B21R1, June 1999.
8. J. W. Betz and K. R. Kolodziejski, "Generalized Theory of GPS Code Tracking Accuracy with an Early-Late Discriminator," to be Submitted to *IEEE Transactions on Aerospace and Electronic Systems*.
9. J. W. Betz, "Effect of Narrowband Interference on GPS Code Tracking Accuracy," *Proceedings of ION 2000 National Technical Meeting*, Institute of Navigation, January 2000.
10. J. W. Betz, "Effect of Jamming on GPS M Code Signal SNIR and Code Tracking Accuracy," *Proceedings of ION 2000 National Technical Meeting*, Institute of Navigation, January 2000. Not currently in the public domain.
11. J. K. Holmes, *Coherent Spread Spectrum Systems*, Krieger Publishing, 1990.
12. P. Fine and W. Wilson, "Tracking Algorithm for GPS Offset Carrier Signals", *Proceedings of ION 1999 National Technical Meeting*, Institute of Navigation, January 1999.
13. J. W. Betz, "Effect of Narrowband Interference on GPS Code Tracking Accuracy," *Proceedings of ION 2000 National Technical Meeting*, Institute of Navigation, January 2000.
14. J. T. Correia, et al., "A Hardware Testbed for Evaluation of the GPS Modernization Modulation Candidates," Proceedings *of ION 2000 National Technical Meeting*, Institute of Navigation, January 2000.
15. L. D. Vittorini, "Lm Channel Models," Viewgraph Presentation Provided to GMSDT, June 1999.
16. S. A. Stephens and J. B. Thomas, "Controlled-Root Formulation for Digital Phase-Locked Loops," *IEEE Trans. on Aerospace and Electronic Systems*, Vol. 31, No. 1, January 1995, pp. 78–95.